10(2013) 409 – 440

Latin American Journal of Solids and Structures
www.lajss.org

Behaviour of stiffened concrete-filled steel composite (CFSC) stub columns

Abstract
This paper investigates the behaviour of axially loaded stiffened concrete-filled steel composite (CFSC) stub columns using the finite element software LUSAS. Modelling accuracy is established by comparing results of the nonlinear analysis and the experimental test. The CFSC stub columns are extensively developed using different special arrangements, number, spacing, and diameters of bar stiffeners with various steel wall thicknesses, concrete compressive strengths, and steel yield stresses. Their effects on the columns behaviour are examined. Failure modes of the columns are also illustrated. It is concluded that the parameters have considerable effects on the behaviour of the columns. An equation is proposed based on the obtained results to predict the ultimate load capacity of the columns. Results are compared with predicted values by the design code EC4, suggested equation of other researchers, and proposed equation of this study which is concluded that the proposed equation can give closer predictions than the others.

Keywords
Stub column, concrete, nonlinear analysis, bar stiffener, ultimate load capacity, ductility.

Alireza Bahrami*
Wan Hamidon Wan Badaruzzaman
Siti Aminah Osman

Department of Civil and Structural Engineering, Universiti Kebangsaan Malaysia, Bangi, Selangor, Malaysia

Received 29 Jun 2012
In revised form 8 Oct 2012

* Author email: bahrami_a_r@yahoo.com

1 INTRODUCTION

The strength and stiffness of concrete-filled steel composite (CFSC) columns are optimised by the location of steel and concrete in their cross-sections. Steel is situated at the outer perimeter where it acts most efficiently in tension and in withstanding bending moments. Also, the stiffness of CFSC columns is considerably increased since the steel lies farthest from the centroid, where it contributes the greatest to the moment of inertia. Concrete makes an ideal core to resist compressive loads [4]. Inward buckling of the steel wall is prevented by the concrete core which leads to the delay of the local buckling of the steel wall. Whilst spalling of the concrete core is prevented by the steel wall. Also, the steel wall eliminates the need for the longitudinal and transverse reinforcements and it behaves as permanent formwork to the concrete core which results in reducing materials and labours costs [10]. The steel consumption in CFSC columns is less than the steel columns leading to cost saving. On the other hand, CFSC columns have structural benefits such as high strength, large stiffness, and high ductility. Also, the surface of concrete is protected from damage by the steel wall in CFSC columns. Simple connections can be utilised between steel floor beams and CFSC columns and extra work is not required to make the columns stiffer in the area of the connection. In CFSC columns, deformations due to shrinkage are negligible and deformations owing to creep are about one third of their reinforced concrete counterparts. By

the use of CFSC columns, several floors can be constructed and construction loadings can be supported before the concrete filling during the construction stage which highlights using CFSC columns as a cost effective structural element in multi-storey buildings. The cross-sectional area of CFSC columns can be reduced owing to higher strength of the columns. Steel plate thickness can be decreased which leads to more savings in weight and material. The use of CFSC columns increases the speed of the construction process of a building in the upper stories which is because of the point that steel elements of higher levels can be fabricated even if concrete has not been filled in the lower column [34]. Moreover, CFSC columns have ecological benefits over reinforced concrete columns: reinforcement and formwork are not used in CFSC columns which brings about a clean construction site; high strength concrete in CFSC columns which does not possess reinforcement can be crushed easily and reutilised as aggregates when the building is demolished; and the steel wall that peels from the concrete core can be reused [32]. The aforementioned advantages of CFSC columns have shown their priority over steel and reinforced concrete columns and have also resulted in their expanding usage in modern construction projects throughout the world.

A high fire resistance can be achieved for CFSC columns compared to hollow steel tubular columns [18]. Although, steel is a highly thermal conductive material, it quickly loses its strength and stiffness under fire exposure [6]. Bailey [3] noted that for steel tubular columns, different fire protection methods may be used to improve the fire resistance which are mostly expensive and do not strengthen the columns. Concrete-infill has been considered as an effective temperature sink which decreases the temperature in the steel wall during fire. Moreover, since the temperature of the concrete core is increased much slower than that of the steel wall, the concrete core can afford proper load capacity even when the steel wall has a high temperature. When a CFSC column is subjected to fire, the different thermal properties of steel and concrete, and the steel wall trapping the concrete core can lead to having higher temperature for the steel wall than the concrete core. The different thermal expansions in the steel wall and the concrete core decrease their interaction. In the initial stage of exposure to fire, the steel wall carries the load [40]. Then, since the steel wall attains critical temperature it yields which is led to the significant decrease of its strength. Therefore, the load is transferred from the steel wall to the concrete core. The concrete core prevents the steel wall from inward buckling. But, after fire exposure, outward buckling can be occurred meaning the local separation of the steel wall and the concrete core, and finally the column fails [22]. Since the fire resistance of CFSC columns is higher than that of hollow steel tubular columns, it is not needed to provide external protection in most cases [38]. However, according to Lua et al. [29], there are several methods for further improvement of the fire resistance of CFSC columns such as using external fire insulation coating, utilising steel reinforcements in the concrete core and using high performance concrete ([16], [22], [25]). Also, adding fibres to concrete is an effective method in order to obtain high performance concrete to attain higher fire resistance ([23], [31]).

A series of research works have been carried out on the behaviour of the CFSC columns. Uy and Patil [46] assessed the use of high strength concrete in steel box columns. 22 high-strength rectangular concrete-filled steel hollow section stub columns with aspect ratios of 1, 1.5, and 2 were tested under axial concentric loading by Liu *et al.* [28]. Han *et al.* [17] experimentally investigated 50 self-consolidating concrete-filled hollow structural steel stub columns subjected to an axial load. Tao *et al.* [42] carried out tests on concrete-filled steel tubular stub columns with inner and outer welded longitudinal steel stiffeners under axial compression. Tests on concrete-filled stiffened thin-walled steel tubular columns were performed by Tao *et al.* [41]. Behaviour and design of axially loaded concrete-filled stainless steel columns were evaluated by Lam and Gardner [24]. The data from 1819 tests on concrete-filled steel tube columns were summarised by Good and Lam [14] and the failure loads of the columns were also compared with the predictions of the code EC4 [11]. The comparison with the code illustrated that the code can be confidently utilised and generally agrees well with the test results. 32 concrete-filled steel tubular stub columns were experimentally studied under axially local compression by Han *et al.* [15]. Tests on concrete-filled composite columns were done by Liew and Xiong [26] to assess the effect of

preload on the axial capacity of the columns. Tao *et al.* [43] conducted experiments on concrete-filled stiffened thin-walled steel tubular columns under axial loading. Tests on concrete-filled double skin columns were carried out under compression by Uenaka *et al.* [45]. Oliveira *et al.* [36] experimentally evaluated passive confinement effect of the steel tube in concrete-filled steel tubular columns. An experimental and analytical investigation on concrete-filled tubes with critical lengths ranging from 131 cm to 467 cm was performed by Muciaccia *et al.* [33]. Uy *et al.* [47] tested short and slender concrete-filled stainless steel tubular columns to investigate their performance under axial compression and combined action of axial force and bending moment. Nonlinear behaviour of concrete-filled steel composite slender columns was studied by Bahrami *et al.* [1] to evaluate and develop different shapes (V, T, L, Line, & Triangular) and number (1 on side & 2 on side) of longitudinal cold-formed steel sheeting stiffeners and also to assess their effects on the structural behaviour of the columns. However, research works on the behaviour of stiffened CFSC stub columns are limited.

This paper deals with the behaviour of the stiffened concrete-filled steel composite (CFSC) stub columns subjected to axial loading. Verification of the proposed three-dimensional (3D) finite element modelling is performed by comparison of the finite element result with the existing experimental result presented by Tao *et al.* [42]. The verification demonstrates that the proposed finite element modelling of this study can accurately predict the behaviour of the columns. The CFSC stub columns are widely developed using different special arrangements, number, spacing, and diameters of bar stiffeners with various steel wall thicknesses, concrete compressive strengths, and steel yield stresses. Extensive parameters are considered in the nonlinear finite element analyses to investigate the behaviour of the columns. The main parameters are: (1) arrangements of bar stiffeners (C1 and C2); (2) number of bar stiffeners (2, 3, and 4); (3) spacing of bar stiffeners (from 50 mm to 150 mm); (4) diameters of bar stiffeners (from 8 mm to 12 mm); (5) steel wall thicknesses (from 2 mm to 3 mm); (6) concrete compressive strengths (from 30 MPa to 50.1 MPa), and (7) steel yield stresses (from 234.3 MPa to 450 MPa). Effects of different number and spacing of the bar stiffeners and also steel wall thicknesses on the ultimate load capacity and ductility of the columns are examined. In addition, effects of various arrangements and diameters of the bar stiffeners, concrete compressive strengths, and steel yield stresses on the ultimate load capacity of the columns are evaluated. Failure modes of the columns are assessed. An equation is also proposed based on the obtained results to predict the ultimate load capacity of the columns. The ultimate load capacities achieved from the nonlinear finite element analyses are compared with predicted values by the design code EC4 [11], equation of other researchers, and proposed equation of this study.

2 FINITE ELEMENT MODELLING

The nonlinear 3D finite element modelling was conducted by the use of the finite element software LUSAS to simulate the CFSC stub columns. The stub column experiment carried out by Tao *et al.* [42] has been chosen for the nonlinear finite element modelling in this paper. The steel wall thickness (t) and cross-section of the column were 2.5 mm and 249 mm × 250.4 mm, respectively, as shown in Figure 1. The length of the column was 750 mm.

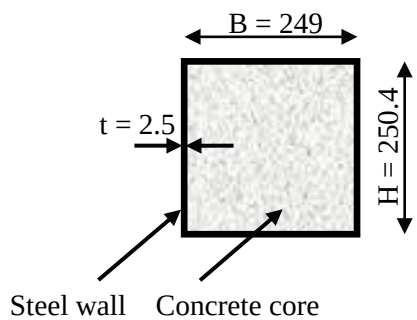

Figure 1 Cross-section of unstiffened CFSC stub column, (unit: mm)

In order to accurately simulate the actual behaviour of the columns, crucial parameters such as finite element type, mesh, concrete-steel interface, boundary conditions, and load application are needed to be taken into account in the simulation of the columns. Meanwhile, constitutive models of the steel wall, steel bar stiffeners, and concrete are important which should be suitably considered in the modelling.

2.1 Finite Element Type, Mesh, Concrete-Steel Interface, Boundary Conditions, and Load Application

The element library of the finite element software LUSAS (Finite Element Analysis Ltd. [12]) was used to select the type of elements for the steel wall and concrete core of the columns in this study. The 6-noded triangular shell element, TSL6, was used for modelling of the steel wall. This is a thin, doubly curved, isoparametric element which can be utilised to model 3D structures. This element can accommodate generally curved geometry with varying thickness and anisotropic and composite material properties. The element formulation takes account of both membrane and flexural deformations. The steel bar stiffeners were modelled by the 3-noded bar element type BRS3. This is an isoparametric bar element in 3D which can accommodate varying cross-sectional area. This element is suitable for modelling stiffening reinforcement with continuum elements. The 10-noded tetrahedral element, TH10, was utilised to model the concrete core. This is a 3D isoparametric solid continuum element capable of modelling curved boundaries. This type of element is a standard volume element of the LUSAS software.

Different finite element mesh sizes were tried to find a reasonable mesh size which can provide accurate results. Consequently, it was uncovered that the mesh size corresponding to 7713 elements can obtain exact results. Therefore, this mesh size was used in the nonlinear finite element analyses to accurately predict the behaviour of the columns. Figure 2 illustrates a typical finite element mesh used herein.

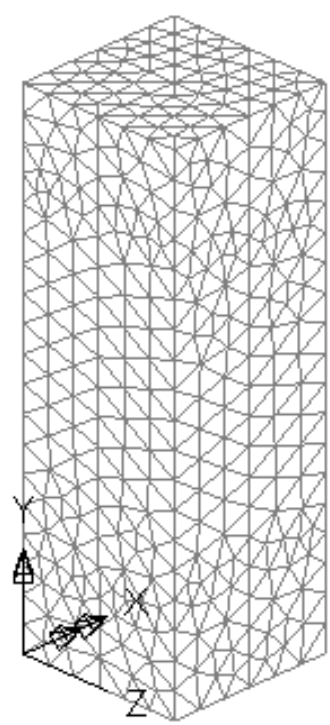

Figure 2 A typical finite element mesh

Slidelines were employed to represent the contact between the concrete core and steel (comprising steel wall and steel bar stiffeners). The slidelines are attributes which can be utilised to model contact surfaces in the finite element software LUSAS. The slideline contact facility is nonlinear and was used in the nonlinear analyses. Slave and master surfaces needed to be correctly selected to provide the contact between surfaces of steel and concrete. If a smaller surface is in contact with a larger surface, the smaller surface can be best selected as the slave surface. If it is not possible to distinguish this point, the body which possesses higher stiffness should be selected as the master surface. It needs to be highlighted that the stiffness of the structure should be considered not just the material. Although, the steel material is stiffer than the concrete material, steel may have less stiffness than the volume of the concrete core herein. As a result, the concrete core and steel surfaces were respectively selected as the master and slave surfaces. This process of choosing master and slave surfaces has been also stated by Dabaon *et al.* [5]. The definition of properties such as friction coefficient is allowed in the slidelines. The friction between two surfaces, the concrete core and steel, is considered so that they can be in contact. The Coulomb friction coefficient in the slidelines was chosen as 0.25. The slidelines allow the concrete core and steel to separate or slide but not to penetrate each other.

Pin-ended supports of the corresponding experiment have been accurately simulated in the finite element modelling in this study. Accordingly, the rotations of the top and bottom surfaces of the columns in the X, Y, and Z directions were considered to be free. Also, the displacements of the top and bottom surfaces in the X and Z directions were restrained. On the other hand, the displacement of the bottom surface in the Y direction was restrained while that of the top surface, in the direction of the applied load and where the load was applied, was set to be free.

The axial loading of the experiment has been appropriately simulated using incremental displacement load with an initial increment of 1 mm applied axially to the top surface of the columns in the negative Y direction.

2.2 Constitutive Models

Materials used in the numerical analysis consist of steel wall, steel bar stiffener, and concrete. Constitutive models of the materials play a vital role in the behaviour of the columns and are presented in the following:

2.2.1 Steel Wall

Modelling of the steel wall has been carried out as an elastic-perfectly plastic material in both tension and compression. The stress-strain curve used for the steel wall is shown in Figure 3(a). The yield stress, modulus of elasticity, and Poisson's ratio of the steel wall have been respectively taken as 234.3 MPa, 208,000 MPa, and 0.247 that are identical to those in the corresponding experiment. Von Mises yield criterion, an associated flow rule, and isotropic hardening have been also utilised in the nonlinear material model.

2.2.2 Steel Bar Stiffener

The uniaxial behaviour of the steel bar stiffener is similar to that of the steel wall. Therefore, it can be simulated by the elastic-perfectly plastic material model (Figure 3(a)). The yield stress and modulus of elasticity of the steel bar stiffener have been considered as 400 MPa and 200,000 MPa, respectively.

2.2.3 Concrete

The compressive strength and modulus of elasticity of concrete have been respectively adopted as 50.1 MPa and 35,100 MPa which are the same as those in the corresponding experiment. Figure 3(b) shows the equivalent uniaxial stress-strain curves for concrete (Ellobody and Young [7, 8]) which have been used in this study to model concrete. The unconfined concrete cylinder compressive strength $f_c = 0.8f_{cu}$ in which f_{cu} is the unconfined concrete cube compressive strength. In accordance with Hu *et al.* [19], the corresponding unconfined strain ε_c is usually around the range of 0.002-0.003. They considered ε_c as 0.002. The same value for ε_c has been also taken in the analysis herein. When concrete is under laterally confining pressure, the confined compressive strength f_{cc} and the corresponding confined strain ε_{cc} are much greater than those of unconfined concrete.

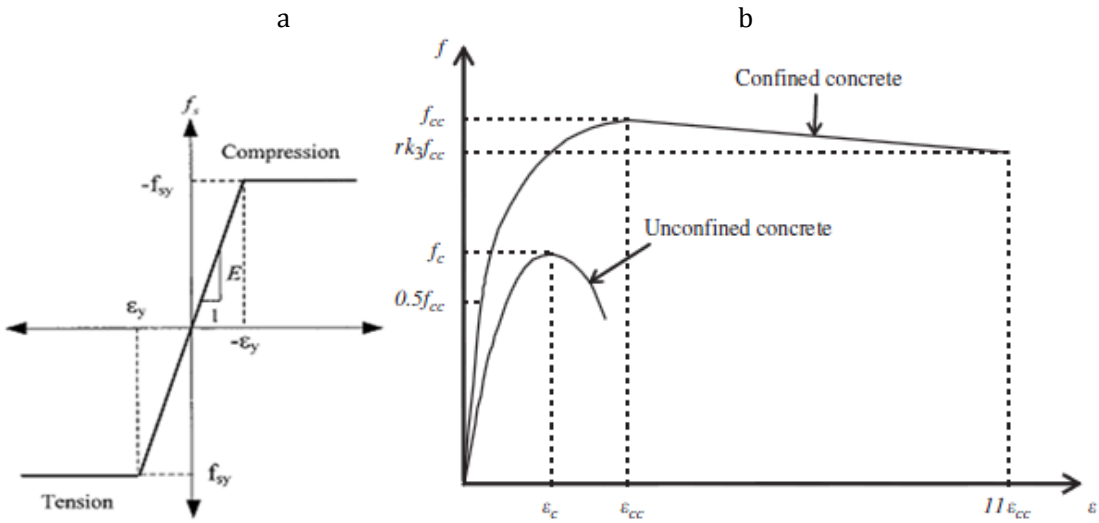

Figure 3 Stress-strain curves: (a) steel, (b) concrete

Equations (1) and (2) have been used to respectively obtain the confined concrete compressive strength f_{cc} and the corresponding confined stain ε_{cc}, as presented by Mander *et al.* [30]:

$$f_{cc} = f_c + k_1 f_1 \tag{1}$$

$$\varepsilon_{cc} = \varepsilon_c\left(1 + k_2 \frac{f_1}{f_c}\right) \tag{2}$$

where f_1 is the lateral confining pressure of the steel wall on the concrete core. The approximate value of f_1 can be interpolated from the values reported by Hu *et al.* [20]. According to Richart *et al.* [37], the factors of k_1 and k_2 have been taken as 4.1 and 20.5, respectively. Since f_1, k_1 and k_2 are known f_{cc} and ε_{cc} can be calculated by the use of Equations (1) and (2). The equivalent uniaxial stress-strain curve for confined concrete (Figure 3(b)) comprises three parts which are needed to be defined. The first part consists of the initially assumed elastic range to the proportional limit stress. The value of the proportional limit stress has been adopted as $0.5f_{cc}$, as recommended by Hu *et al.* [20]. The empirical Equation (3) has been used to determine the initial Young's modulus of confined concrete E_{cc}. The Poisson's ratio υ_{cc} of confined concrete has been considered as 0.2.

$$E_{cc} = 4700\sqrt{f_{cc}}\ \text{MPa}. \tag{3}$$

The second part includes the nonlinear portion which starts from the proportional limit stress $0.5f_{cc}$ to the confined concrete strength f_{cc}. The common Equation (4) presented by Saenz [39] can be used to determine this part. The values of uniaxial stress f and strain ε are the unknowns of the equation which define this part of the curve. The strain values ε have been considered between the proportional strain ($0.5f_{cc}/E_{cc}$), and the confined strain ε_{cc} which corresponds to the confined concrete strength. Equation (4) can be used to determine the stress values f by assuming the strain values ε.

$$f = \frac{E_{cc}\varepsilon}{1+(R+R_E-2)\left(\frac{\varepsilon}{\varepsilon_{cc}}\right)-(2R-1)\left(\frac{\varepsilon}{\varepsilon_{cc}}\right)^2+R\left(\frac{\varepsilon}{\varepsilon_{cc}}\right)^3} \tag{4}$$

in which R_E and R are:

$$R_E = \frac{E_{cc}\varepsilon_{cc}}{f_{cc}}$$

$$R = \frac{R_E(R_\sigma-1)}{(R_\varepsilon-1)^2}-\frac{1}{R_\varepsilon}$$

The constants R_ε and R_σ have been adopted as 4 in this study, as reported by Hu and Schnobrich [21]. The third part of the curve is the descending part which is between f_{cc} and rk_3f_{cc} with the corresponding strain of $11\varepsilon_{cc}$. k_3 is the reduction factor dependent on the H/t ratio. Empirical equations proposed by Hu *et al.* [20] can be utilised to determine the approximate value of k_3. To consider the effect of different concrete strengths, the reduction factor r was introduced by Ellobody *et al.* [9] on the basis of the experimental study carried out by Giakoumelis and Lam [13]. According to Tomii [44] and also Mursi and Uy [35], the value of r has been adopted as 1.0 for concrete with cube strength f_{cu} equal to 30 MPa and as 0.5 for concrete with f_{cu} greater than or equal to 100 MPa. The value of r for concrete cube strength between 30 MPa and 100 MPa has been calculated by the use of linear interpolation.

2.3 Modelling Verification

Verification of the finite element modelling was carried out by comparison of the modelling result with the experimental result reported by Tao *et al.* [42]. Figure 4 demonstrates that the load-normalised axial shortening curves obtained from the modelling and corresponding experiment agree well with each other. The obtained ultimate load capacity from the finite element analysis is 3325 kN while that from the experiment is 3230 kN. Accordingly, their difference is only 2.9% which uncovers the accuracy of the modelling. As a consequence, the proposed 3D finite element modelling can accurately predict the behaviour of the columns herein.

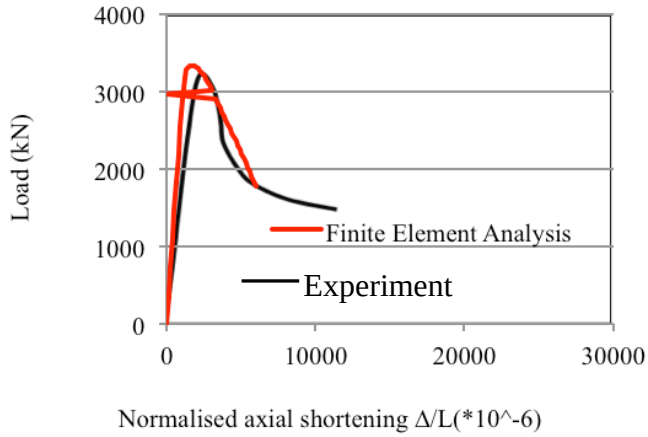

Figure 4 Load versus normalised axial shortening curves for the CFSC stub columns

3 NUMERICAL ANALYSIS

Because the accuracy of the proposed 3D finite element modelling of this study was demonstrated, the method was used for the nonlinear analysis of stub columns of same size and cross-section as that tested by Tao *et al.* [42] but with bar stiffeners. Each of the CFSC stub columns was accurately modelled based on the described modelling features. Figure 5 illustrates details of the stiffened CFSC stub columns which were analysed by the use of nonlinear finite element method. As can be seen from Figure 5 (a, b), 2 different special arrangements of the bar stiffeners namely C1 and C2 are considered in this study. Also, various number (2, 3, and 4) and spacing of the bar stiffeners (50 mm, 100 mm, and 150 mm) are adopted in the columns in which 2 typical elevations are shown in Figure 5 (c, d). In addition, typical finite element meshes of the stiffened CFSC columns are illustrated in Figure 6.

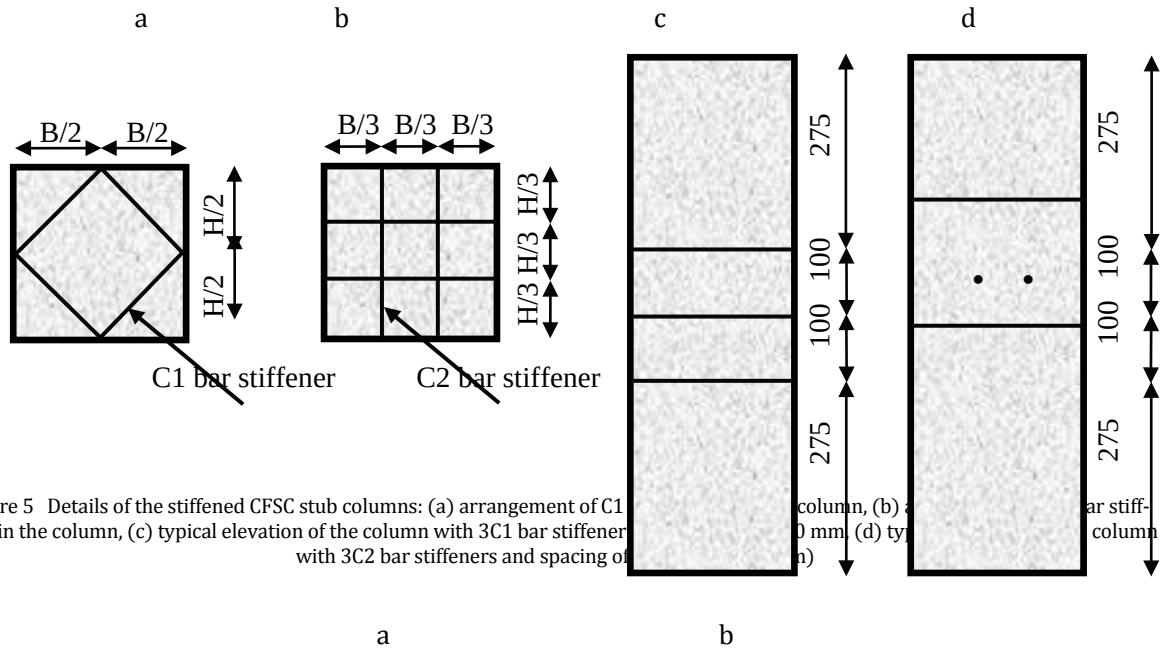

Figure 5 Details of the stiffened CFSC stub columns: (a) arrangement of C1 ... column, (b) ... ar stiffener in the column, (c) typical elevation of the column with 3C1 bar stiffener ... 0 mm, (d) typ... column with 3C2 bar stiffeners and spacing of ... n)

a b

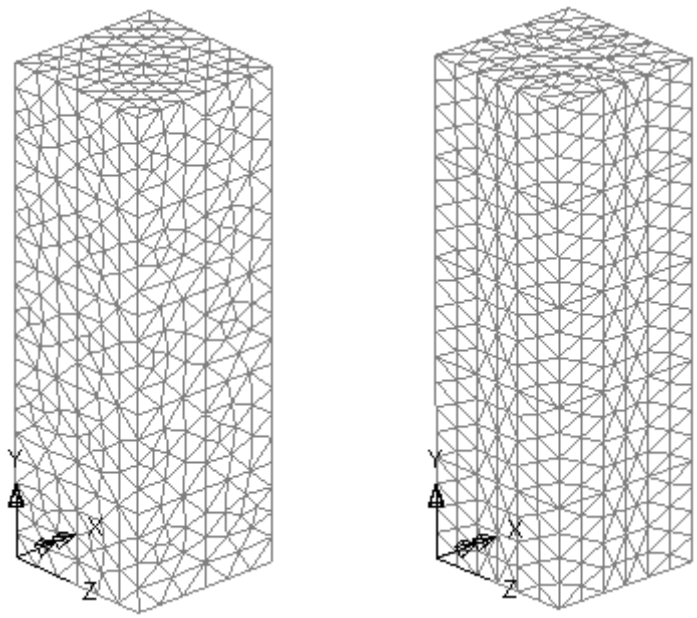

Figure 6 Typical finite element meshes of the stiffened CFSC stub columns: (a) column with 4C1 bar stiffeners and spacing of 150 mm, (c) column with 4C2 bar stiffeners and spacing of 150 mm

4 RESULTS AND DISCUSSION

Table 1 summarises specifications and obtained ultimate load capacities of the analysed CFSC stub columns. C1 and C2 in the column labels represent the columns with different special arrangements of the bar stiffeners as illustrated in Figure 5 (a, b). The first four numbers following C1 and C2 respectively denote the steel wall thickness t (mm), diameter of bar stiffener D (mm), steel wall yield stress f_y (MPa), and concrete compressive strength f_c (MPa). Also, the number before the parentheses is the number of the bar stiffeners and the number in the parentheses represents the centre-to-centre spacing (mm) between the bar stiffeners. Moreover, the load eccentricity (e) for those eccentrically loaded columns is added to the columns labels as the last number after the parentheses, i.e. 30 and 60 respectively stand for the load eccentricities of 30 mm and 60 mm. Effects of various parameters on the behaviour of the columns are presented in the following sections.

Table 1 Specifications and ultimate load capacities (N_u) of the columns

No.	Column label	Steel wall t (mm)	Bar stiffener D (mm)	Steel wall f_y (MPa)	Concrete f_c (MPa)	N_u (kN)
1	C1-2.5-10-234-50-4(50)	2.5	10	234.3	50.1	3760
2	C1-2.5-10-234-50-3(50)	2.5	10	234.3	50.1	3661

3	C1-2.5-10-234-50-2(50)	2.5	10	234.3	50.1	3517
4	C1-2.5-10-234-50-4(100)	2.5	10	234.3	50.1	3656
5	C1-2.5-10-234-50-3(100)	2.5	10	234.3	50.1	3557
6	C1-2.5-10-234-50-2(100)	2.5	10	234.3	50.1	3424
7	C1-2.5-10-234-50-4(150)	2.5	10	234.3	50.1	3579
8	C1-2.5-10-234-50-3(150)	2.5	10	234.3	50.1	3486
9	C1-2.5-10-234-50-2(150)	2.5	10	234.3	50.1	3359
10	C2-2.5-10-234-50-4(50)	2.5	10	234.3	50.1	3668
11	C2-2.5-10-234-50-3(50)	2.5	10	234.3	50.1	3583
12	C2-2.5-10-234-50-2(50)	2.5	10	234.3	50.1	3473
13	C2-2.5-10-234-50-4(100)	2.5	10	234.3	50.1	3575
14	C2-2.5-10-234-50-3(100)	2.5	10	234.3	50.1	3499
15	C2-2.5-10-234-50-2(100)	2.5	10	234.3	50.1	3398
16	C2-2.5-10-234-50-4(150)	2.5	10	234.3	50.1	3510
17	C2-2.5-10-234-50-3(150)	2.5	10	234.3	50.1	3445
18	C2-2.5-10-234-50-2(150)	2.5	10	234.3	50.1	3348
19	C1-3-10-234-50-4(50)	3	10	234.3	50.1	3905
20	C1-2-10-234-50-4(50)	2	10	234.3	50.1	3596
21	C1-3-10-234-50-3(50)	3	10	234.3	50.1	3793
22	C1-2-10-234-50-3(50)	2	10	234.3	50.1	3525
23	C1-3-10-234-50-2(50)	3	10	234.3	50.1	3665
24	C1-2-10-234-50-2(50)	2	10	234.3	50.1	3368
25	C2-3-10-234-50-4(50)	3	10	234.3	50.1	3825
26	C2-2-10-234-50-4(50)	2	10	234.3	50.1	3516
27	C2-3-10-234-50-3(50)	3	10	234.3	50.1	3732
28	C2-2-10-234-50-3(50)	2	10	234.3	50.1	3437
29	C2-3-10-234-50-2(50)	3	10	234.3	50.1	3622
30	C2-2-10-234-50-2(50)	2	10	234.3	50.1	3320
31	C1-2.5-12-234-50-4(50)	2.5	12	234.3	50.1	3804
32	C1-2.5-8-234-50-4(50)	2.5	8	234.3	50.1	3695
33	C1-2.5-12-234-50-3(50)	2.5	12	234.3	50.1	3721
34	C1-2.5-8-234-50-3(50)	2.5	8	234.3	50.1	3597

Table 1 continued

No.	Column label	Steel wall t (mm)	Bar stiffener D (mm)	Steel wall f_y (MPa)	Concrete f_c (MPa)	N_u (kN)
35	C1-2.5-12-234-50-2(50)	2.5	12	234.3	50.1	3544
36	C1-2.5-8-234-50-2(50)	2.5	8	234.3	50.1	3486

37	C2-2.5-12-234-50-4(50)	2.5	12	234.3	50.1	3719
38	C2-2.5-8-234-50-4(50)	2.5	8	234.3	50.1	3622
39	C2-2.5-12-234-50-3(50)	2.5	12	234.3	50.1	3661
40	C2-2.5-8-234-50-3(50)	2.5	8	234.3	50.1	3505
41	C2-2.5-12-234-50-2(50)	2.5	12	234.3	50.1	3506
42	C2-2.5-8-234-50-2(50)	2.5	8	234.3	50.1	3438
43	C1-2.5-10-234-50-4(50)-30	2.5	10	234.3	50.1	3086
44	C1-2.5-10-234-50-4(50)-60	2.5	10	234.3	50.1	2425
45	C1-2.5-10-234-50-4(100)-30	2.5	10	234.3	50.1	2926
46	C1-2.5-10-234-50-4(100)-60	2.5	10	234.3	50.1	2225
47	C1-2.5-10-234-40-4(50)	2.5	10	234.3	40	3138
48	C1-2.5-10-234-30-4(50)	2.5	10	234.3	30	2520
49	C1-2.5-10-234-40-3(50)	2.5	10	234.3	40	3063
50	C1-2.5-10-234-30-3(50)	2.5	10	234.3	30	2449
51	C1-2.5-10-234-40-2(50)	2.5	10	234.3	40	2942
52	C1-2.5-10-234-30-2(50)	2.5	10	234.3	30	2347
53	C2-2.5-10-234-40-4(50)	2.5	10	234.3	40	3077
54	C2-2.5-10-234-30-4(50)	2.5	10	234.3	30	2468
55	C2-2.5-10-234-40-3(50)	2.5	10	234.3	40	3021
56	C2-2.5-10-234-30-3(50)	2.5	10	234.3	30	2446
57	C2-2.5-10-234-40-2(50)	2.5	10	234.3	40	2909
58	C2-2.5-10-234-30-2(50)	2.5	10	234.3	30	2329
59	C1-2.5-10-450-50-4(50)	2.5	10	450	50.1	4375
60	C1-2.5-10-350-50-4(50)	2.5	10	350	50.1	4102
61	C1-2.5-10-450-50-3(50)	2.5	10	450	50.1	4219
62	C1-2.5-10-350-50-3(50)	2.5	10	350	50.1	3976
63	C1-2.5-10-450-50-2(50)	2.5	10	450	50.1	4067
64	C1-2.5-10-350-50-2(50)	2.5	10	350	50.1	3853
65	C2-2.5-10-450-50-4(50)	2.5	10	450	50.1	4257
66	C2-2.5-10-350-50-4(50)	2.5	10	350	50.1	4011
67	C2-2.5-10-450-50-3(50)	2.5	10	450	50.1	4104
68	C2-2.5-10-350-50-3(50)	2.5	10	350	50.1	3906

Table 1 continued

No.	Column label	Steel wall t (mm)	Bar stiffener D (mm)	Steel wall f_y (MPa)	Concrete f_c (MPa)	N_u (kN)
69	C2-2.5-10-450-50-2(50)	2.5	10	450	50.1	4042

70	C2-2.5-10-350-50-2(50)	2.5	10	350	50.1	3807

4.1 Effects of Arrangement and Number of Bar Stiffeners on Ultimate Load Capacity

The CFSC stub columns with two different special arrangements of bar stiffeners, C1 and C2, (Figure 5(a, b)) and various number of the bar stiffeners (2, 3, and 4) were analysed to investigate their effects on the behaviour of the columns. These effects on the ultimate load capacity are illustrated in Figure 7. Table 1 also summarises the corresponding ultimate load capacity values of the curves.

As can be seen from the figure and table, the use of the bar stiffeners increases the ultimate load capacity of the unsiffened CFSC stub column. As an example, the ultimate load capacity of the unstiffened column is 3325 kN which increases to 3760 kN by the use of 4C1 bar stiffeners (C1-2.5-10-234-50-4(50)), an improvement of 13.1%. Also, using 4C2 bar stiffeners (C2-2.5-10-234-50-4(50)) leads to the ultimate load capacity of 3668 kN which is 10.3% higher than that of the unstiffened column. Therefore, the use of C1 bar stiffeners uncovered to be more effective on the increase of the ultimate load capacity of the unstiffened CFSC columns than C2 bar stiffeners. Moreover, as the number of the bar stiffeners is enhanced the ultimate load capacity is improved. For instance, the ultimate load capacity of the column with 2C1 bar stiffeners and spacing of 100 mm is 3424 kN (C1-2.5-10-234-50-2(100)) which is enhanced to 3656 kN (C1-2.5-10-234-50-4(100)) by the use of 4C1 bar stiffeners and the same bar spacing, an increase of 6.8%.

4.2 Effect of Spacing of Bar Stiffeners on Ultimate Load Capacity

To investigate the effect of spacing of bar stiffeners on the behaviour of the CFSC stub columns, three different bar spacing of 50 mm, 100 mm, and 150 mm were considered in the analyses. Figure 8 indicates this effect on the ultimate load capacity of the columns. In accordance with the figure and Table 1, the ultimate load capacity is increased by the decrease of spacing of the bar stiffeners. For example, by the decrease of spacing of the bar stiffeners from 150 mm to 50 mm with the same number of the bar stiffeners the ultimate load capacity is enhanced from 3486 kN (C1-2.5-10-234-50-3(150)) to 3661 kN (C1-2.5-10-234-50-3(50)), an increase of 5%.

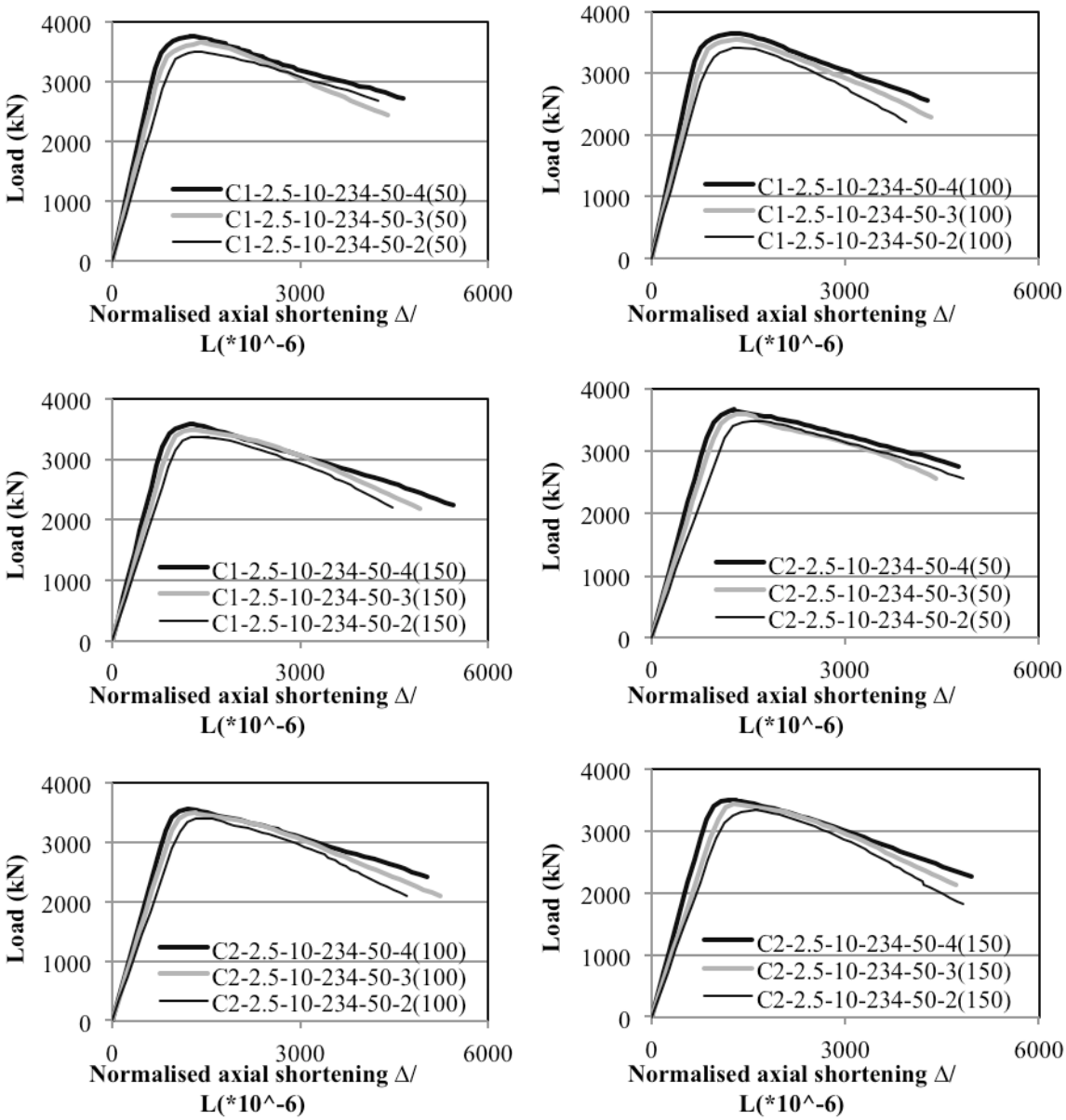

Figure 7 Effects of arrangement and number of bar stiffeners on ultimate load capacity

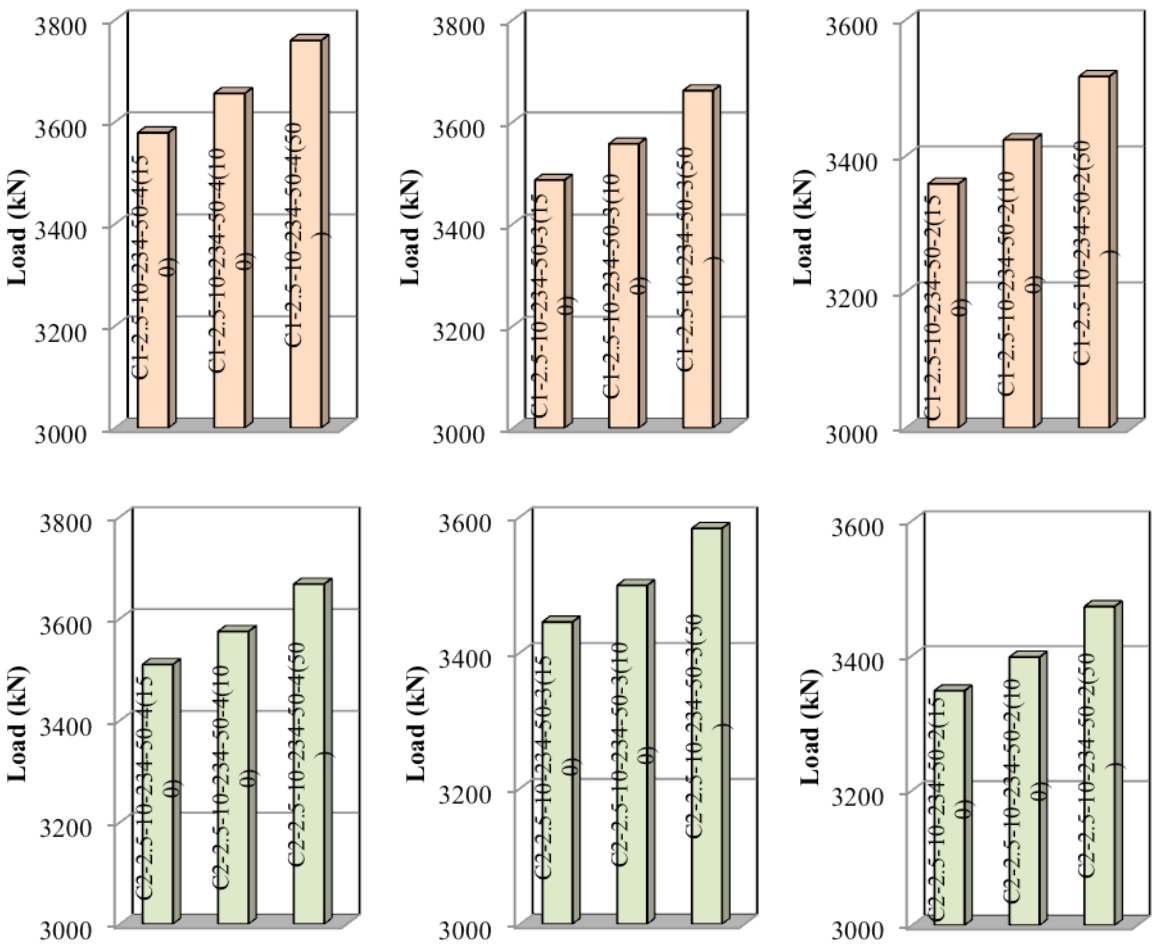

Figure 8 Effects of spacing of bar stiffeners on ultimate load capacity

4.3 Effect of Steel Wall Thickness on Ultimate Load Capacity

The effect of steel wall thickness on the behaviour of the CFSC stub columns was examined by analysing the columns with three different steel wall thicknesses of 2 mm, 2.5 mm, and 3 mm and C1 and C2 bar stiffeners. The results are shown in Figure 9. As can be realised from the figure and Table 1, the increase of the steel wall thickness enhances the ultimate load capacity. As an example, the ultimate load capacity of the column with the same number and spacing of C2 bar stiffeners is increased from 3320 kN (C2-2-10-234-50-2(50)) to 3622 kN (C2-3-10-234-50-2(50)) respectively for the steel wall thicknesses of 2 mm and 3 mm, an improvement of 9.1%.

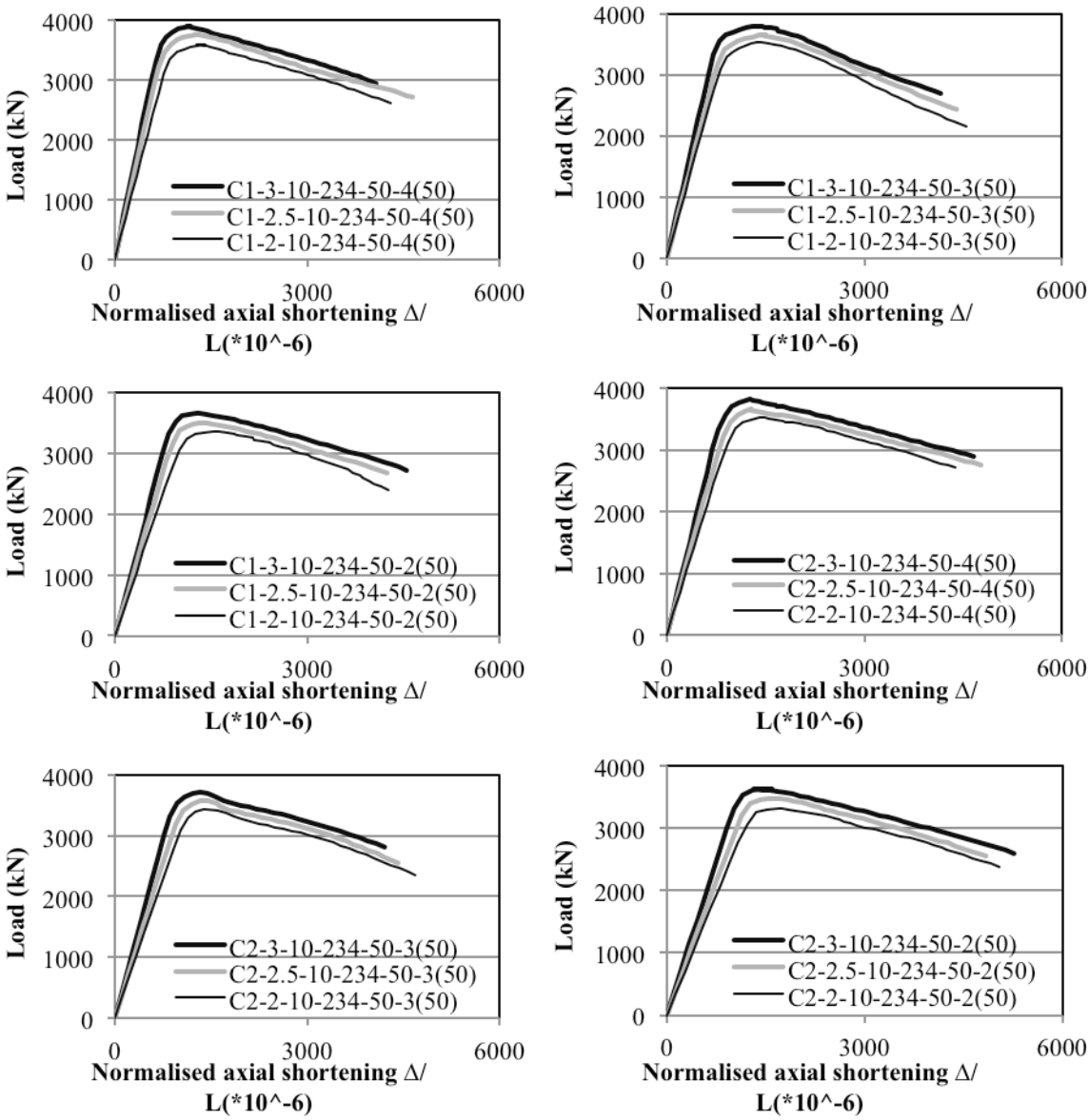

Figure 9 Effect of steel wall thickness on ultimate load capacity

4.4 Effect of Diameter of Bar Stiffeners on Ultimate Load Capacity

Three different diameters of bar stiffeners (8 mm, 10 mm, and 12 mm) were used in the analyses to uncover the effect of diameter of the bar stiffeners on the ultimate load capacity of the CFSC stub columns. Figure 10 illustrates the results. According to the figure and Table 1, larger diameter of the bar stiffeners results in higher ultimate load capacity. For instance, if the diameter of the bar stiffeners is enhanced from 8 mm to 12 mm for the same number and spacing of the bar stiffeners, the ultimate load capacity is increased from 3505 kN (C2-2.5-8-234-50-3(50)) to 3661 kN (C2-2.5-12-234-50-3(50)), an enhancement of 4.5%.

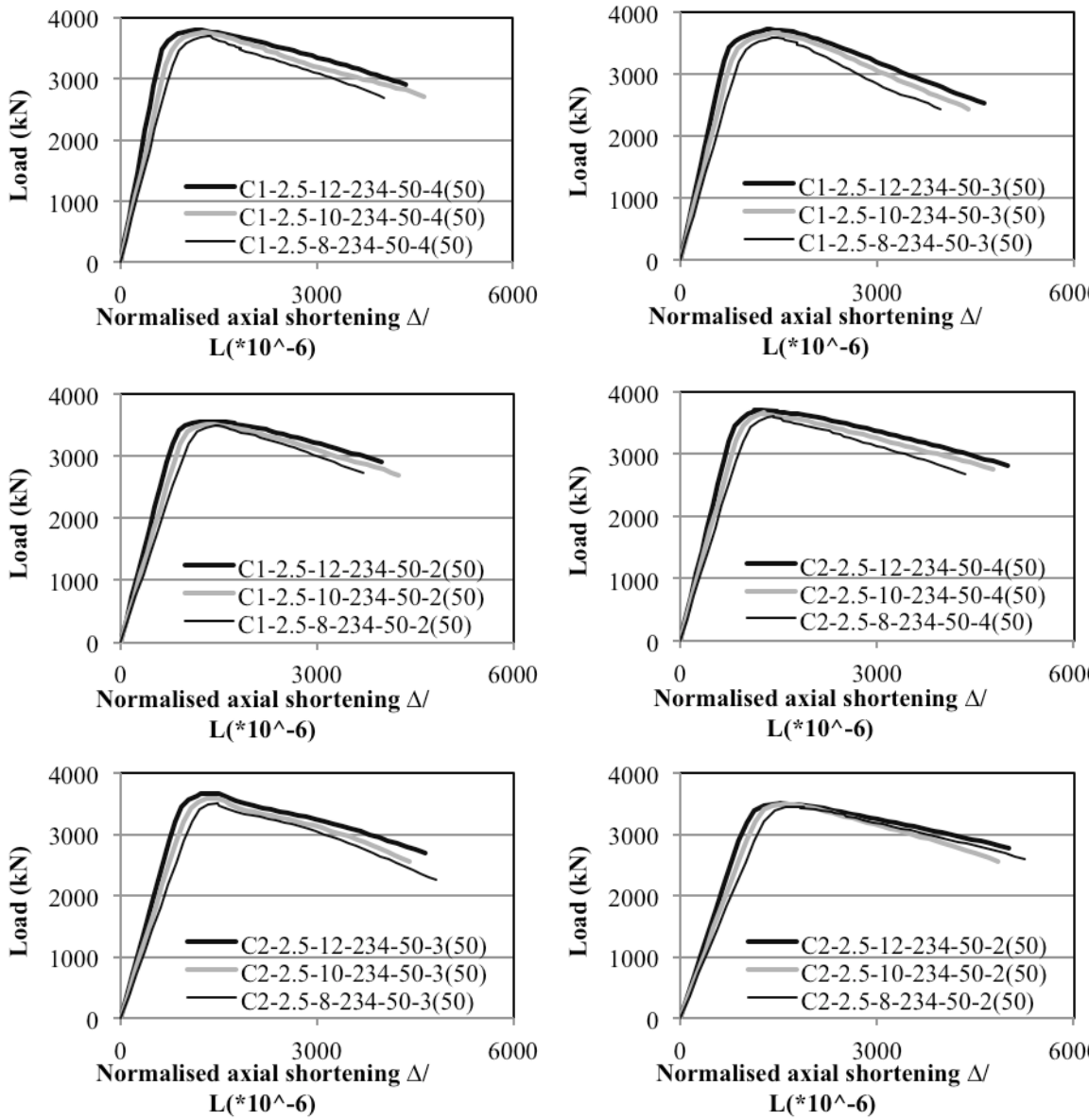

Figure 10 Effect of diameter of bar stiffeners on ultimate load capacity

4.5 Effect of Number and Spacing of Bar Stiffeners on Ductility

In order to assess the ductility of the columns, a ductility index (DI) defined by Lin and Tsai [27] has been utilised in this paper. Equation (5) is the ductility index:

$$DI = \frac{\varepsilon_{85\%}}{\varepsilon_y} \tag{5}$$

where $\varepsilon_{85\%}$ is the nominal axial shortening (Δ/L) corresponding to the load which falls to its 85% of the ultimate load capacity and ε_y is $\varepsilon_{75\%}/0.75$ in which $\varepsilon_{75\%}$ is the nominal axial shortening corresponding

to the load that obtains 75% of the ultimate load capacity. The values of $\varepsilon_{85\%}$ and ε_y can be taken from Figure 7. Effects of number and spacing of the bar stiffeners on the ductility are demonstrated in Figure 11.

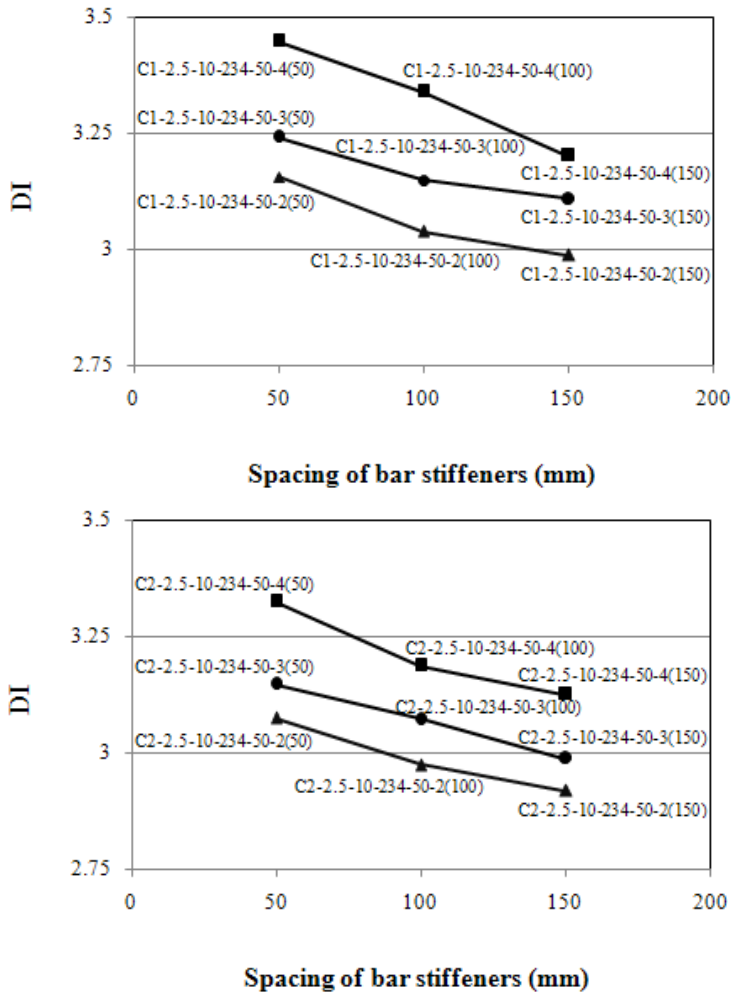

Figure 11 Effects of number and spacing of bar stiffeners on ductility

The ductility of the unstiffened column can be determined as 2.85 from Figure 4 and using Equation (5). The use of 4C1 bar stiffeners (C1-2.5-10-234-50-4(50)) and 4C2 bar stiffeners (C2-2.5-10-234-50-4(50)) in the unstiffened column improves the ductility of the column from 2.85 to 3.447 and 3.325 (Figure 11) respectively, which represent the maximum ductility increases of 20.9% and 16.7%, respectively.

On the other hand, as the number of the bar stiffeners increases the ductility of the columns enhances (Figure 11). For example, by the increase of the number of the bar stiffeners from 2 to 4 for the same bar stiffeners spacing of 100 mm, the ductility improves from 2.974 (C2-2.5-10-234-50-2(100)) to 3.187 (C2-2.5-10-234-50-4(100)), an improvement of 7.2%.

Also, the ductility of the columns is enhanced by the decrease of the bar stiffeners spacing (Figure 11). For instance, the ductility of the column C2-2.5-10-234-50-4(150) is 3.125 which is increased to

3.325 (C2-2.5-10-234-50-4(50)) respectively for the stiffeners spacing of 150 mm and 50 mm, an enhancement of 6.4%.

4.6 Effects of Thickness of Steel Wall on Ductility

Equation (5) of the section 4.5 has been also used to evaluate the effect of steel wall thickness on the ductility of the columns. Figure 12 indicates this effect on the ductility of the columns. The ductility is improved by the increase of the steel wall thickness (Figure 12). As an example, the enhancement of the steel wall thickness from 2 mm to 3 mm enhances the ductility of the column C2-2-10-234-50-2(50) from 2.979 to 3.225 (C2-3-10-234-50-2(50)), an improvement of 8.3%.

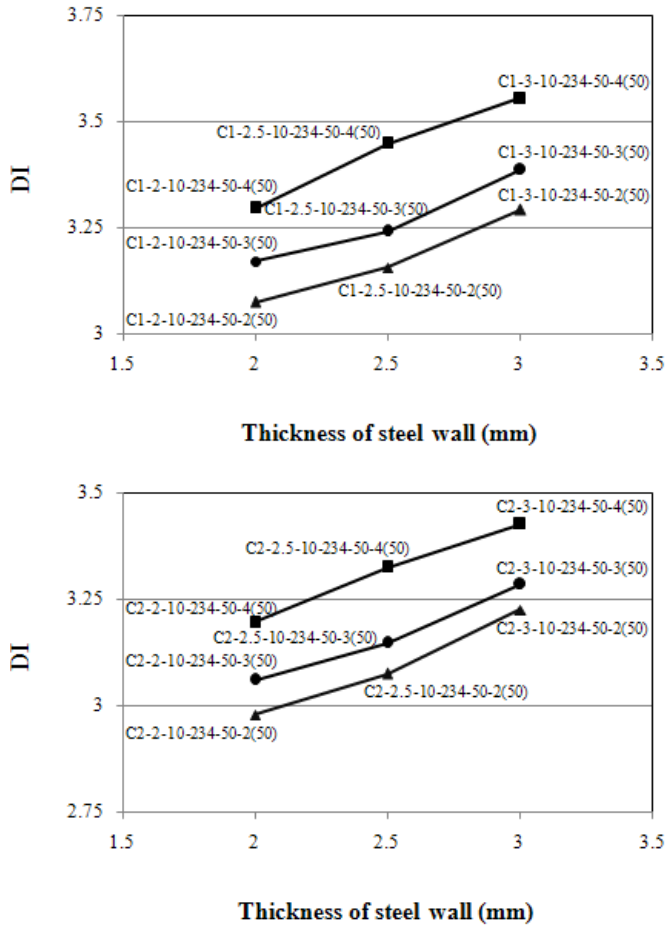

Figure 12 Effect of thickness of steel wall on ductility

4.7 Effect of Load Eccentricity on Ultimate Load Capacity

Two different load eccentricities of 30 mm and 60 mm were taken in the nonlinear analyses of the columns with C1-4(50) and C1-4(100) bar stiffeners to examine the effect of load eccentricity on the ultimate load capacity of the columns. Figure 13 illustrates this effect and Table 1 summarises its ultimate load capacity values. As it is evident from the figure and table, the load eccentricity increase adversely affects the ultimate load capacity. For example, enhancement of the load eccentricity from 30 mm (C1-2.5-10-234-50-4(50)-30) to 60 mm (C1-2.5-10-234-50-4(50)-60), reduces the ultimate load capacity from 3086 kN to 2425 kN, a reduction of 21.4%.

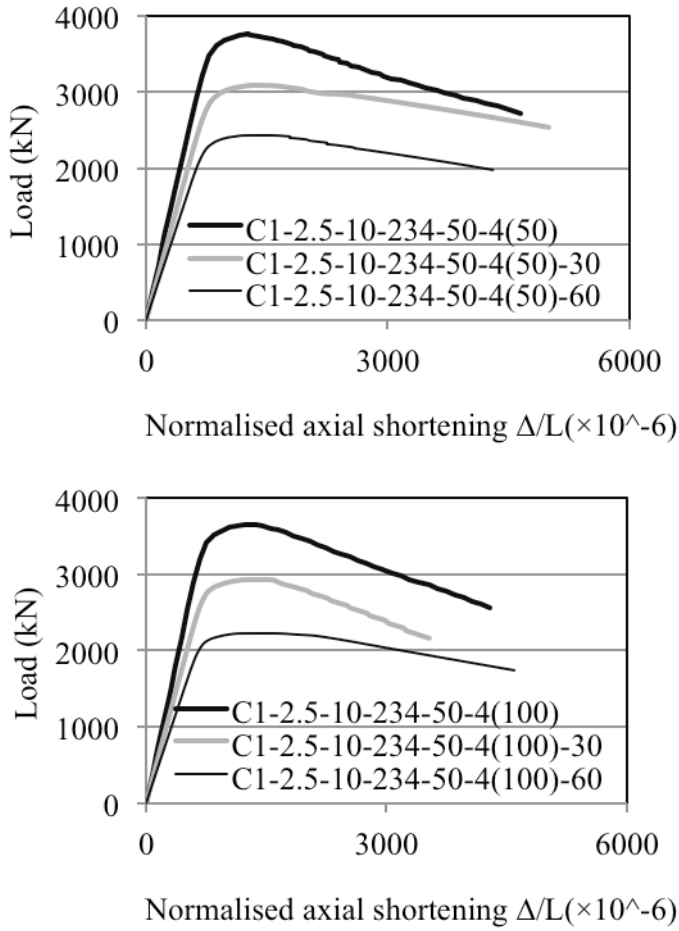

Figure 13 Effect of load eccentricity on ultimate load capacity

4.8 Effect of Concrete Compressive Strength on Ultimate Load Capacity

The effect of various concrete compressive strengths (30 MPa, 40 MPa, and 50.1 MPa) on the ultimate load capacity of the columns is shown in Figure 14 along with their corresponding values in Table 1. It is obvious from the figure and table that the higher concrete compressive strength leads to higher ultimate load capacity of the columns. For example, as the concrete compressive strength is increased from 30 MPa to 50.1 MPa, the ultimate load capacity of the column C2-2.5-10-234-30-3(50) is enhanced from 2446 kN to 3583 kN (C2-2.5-10-234-50-3(50)), an enhancement of 46.5%.

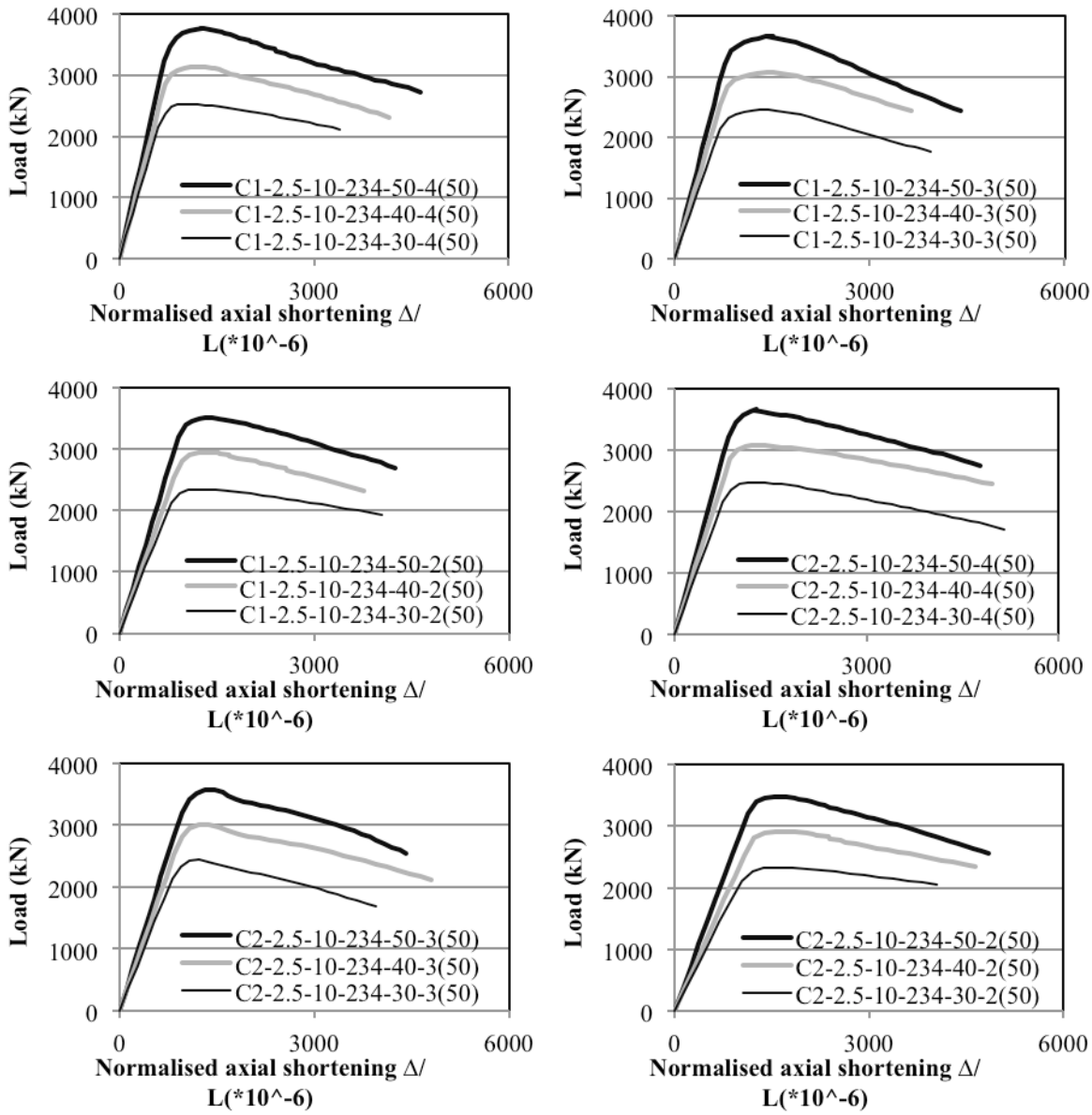

Figure 14 Effect of concrete compressive strength on ultimate load capacity

4.9 Effect of Steel Yield Stress on Ultimate Load Capacity

Figure 15 demonstrates the effect of different steel yield stresses (234.3 MPa, 350 MPa, and 450 MPa) on the ultimate load capacity of the columns. According to the figure and Table 1, the increase of the steel yield stress results in higher ultimate load capacity of the columns. For instance, the ultimate load capacity of the column C2-2.5-10-234-50-4(50) is 3668 kN which is enhanced to 4257 (C2-2.5-10-450-50-4(50)) by the enhancement of the steel yield stress from 234.3 MPa to 450 MPa, an increase of 16.1%.

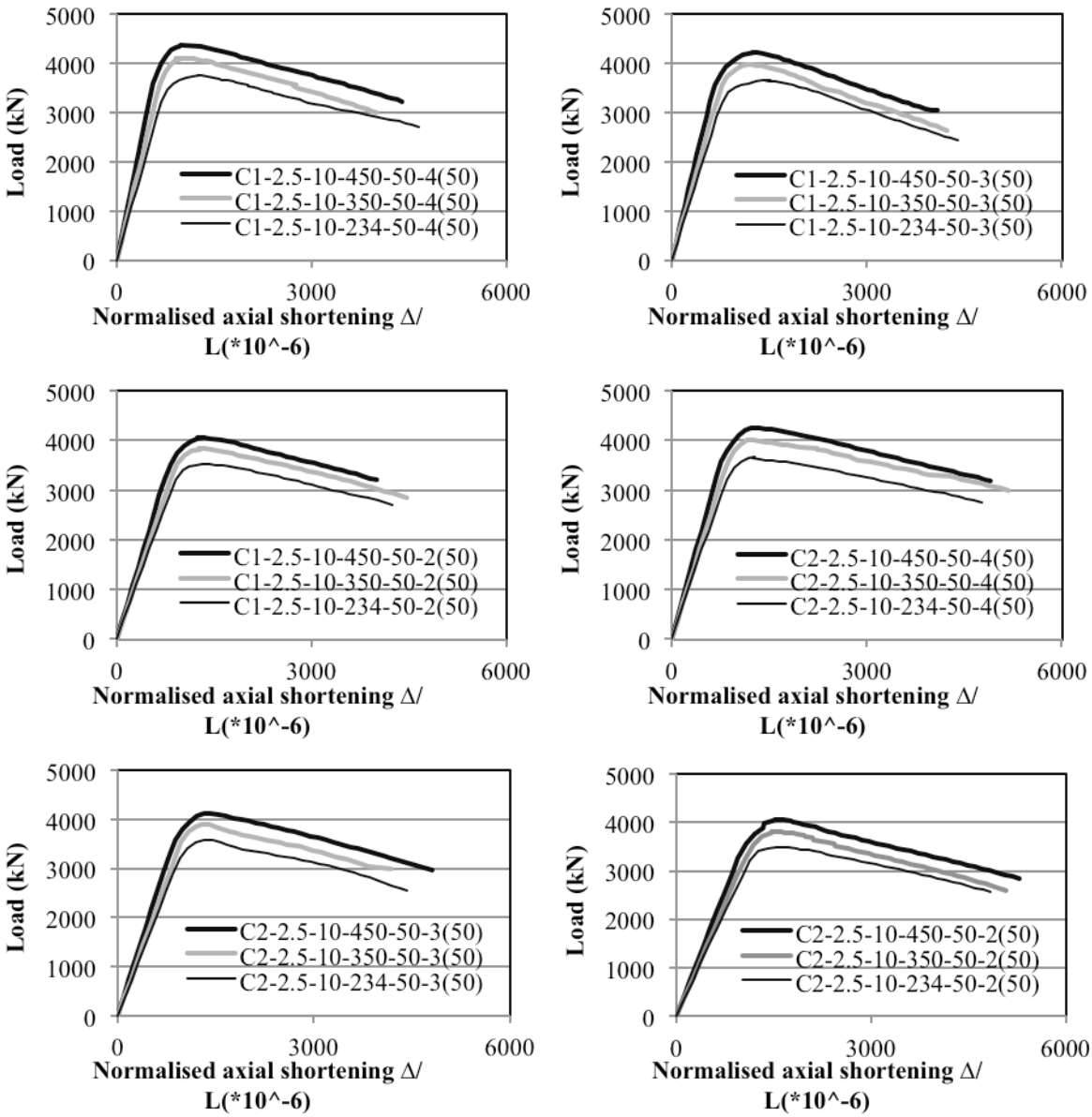

Figure 15 Effect of steel yield stress on ultimate load capacity

4.10 Ultimate load capacity prediction

Typical failure modes of the stiffened CFSC stub columns are illustrated in Figures 16 and 17. As can be seen from the figures, the failure modes of the columns were identified as concrete crushing about their mid-height where local buckling of the steel wall was induced. Also, the in-filled concrete prevented the steel wall from the buckling inward.

Also, it can be noted that the increase of the ultimate load capacity and ductility due to the use of the bar stiffeners, increase of the number of the bar stiffeners, decrease of spacing of the bar stiffeners, enhancement of the steel wall thickness, or increase of diameter of the bar stiffeners can be owing to the enhancement of the confinement effect of the steel wall on the concrete core. This improved con-

finement effect delays the local buckling of the steel wall which leads to the increase of the ultimate load capacity and ductility.

a b c

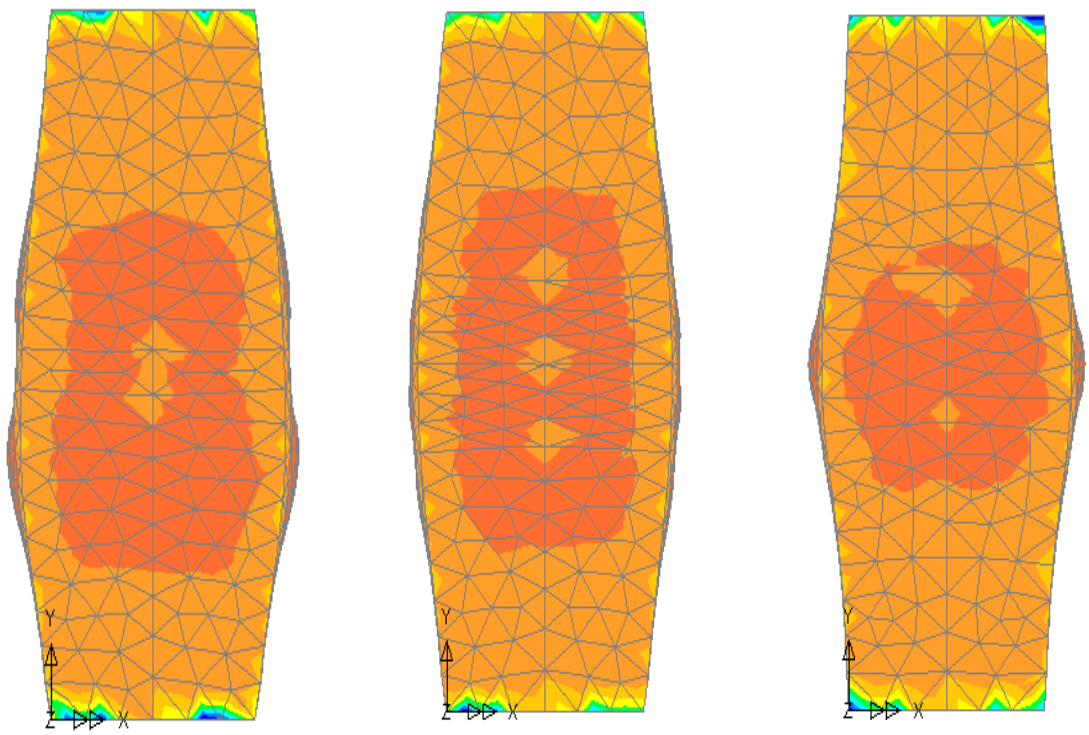

Figure 16 Typical failure modes of the stiffened CFSC stub columns with C1 bar stiffener: (a) 2 bar stiffeners with spacing of 50 mm, (b) 3 bar stiffeners with spacing of 100 mm, (c) 4 bar stiffeners with spacing of 150 mm

a b c

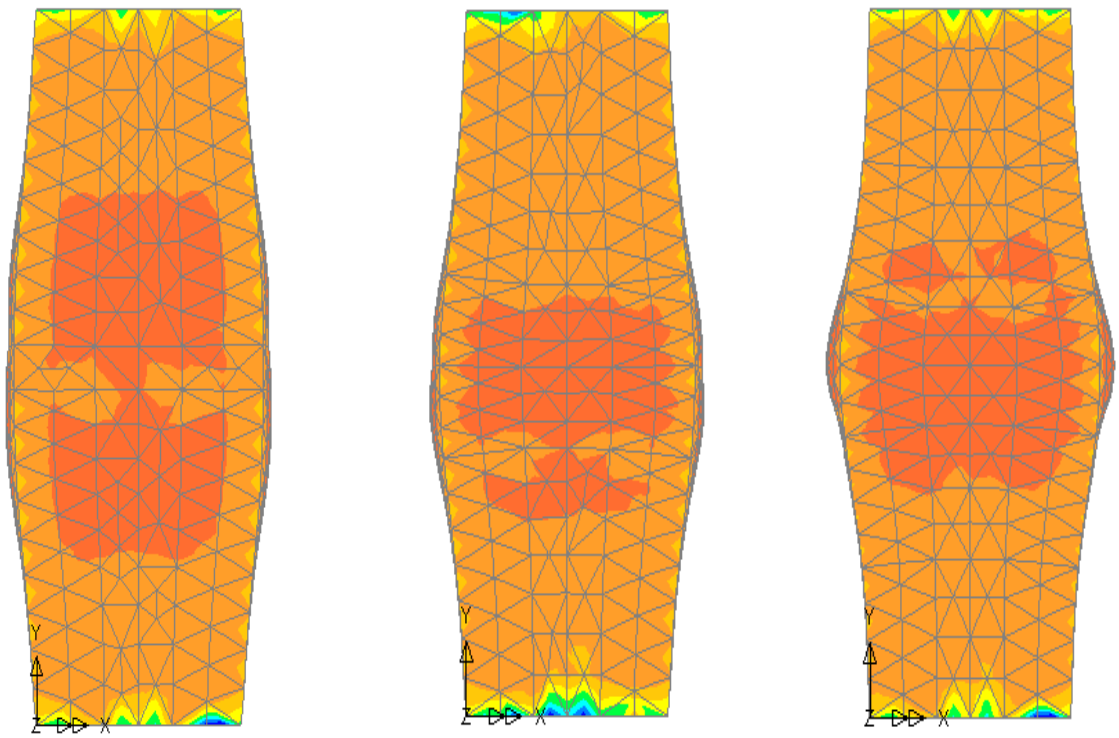

Figure 17 Typical failure modes of the stiffened CFSC stub columns with C2 bar stiffener: (a) 2 bar stiffeners with spacing of 50 mm, (b) 3 bar stiffeners with spacing of 100 mm, (c) 4 bar stiffeners with spacing of 150 mm

4.11 Failure Modes of Stiffened CFSC Columns

EC4 [11] is one of the popular international standards in composite construction which is used throughout the world. According to EC4 [11], the ultimate load capacity of a square or rectangular CFSC stub column can be calculated from Equation (6):

$$N_{\mathrm{pl,Rd}} = A_a f_{yd} + A_c f_{cd} \tag{6}$$

where A_a and A_c are cross-sectional areas of steel and concrete respectively, and also f_{yd} and f_{cd} are yield stress of the steel wall and compressive strength of the concrete core, respectively. The predicted ultimate load capacities based on EC4 [11], $N_{\mathrm{pl,Rd}}$, are listed in Table 2 and compared with the values obtained from the nonlinear analyses of the columns, N_u. SD and COV in Table 2 respectively stand for standard deviation and coefficient of variation determined for the ultimate load capacity values in the table. In accordance with the table, a mean ratio ($N_{\mathrm{pl,Rd}}/N_u$) of 0.949 is obtained with a COV of 0.035 which uncovers that EC4 [11] gives the ultimate load capacity by 5.1% lower than the results obtained from the nonlinear analyses.

On the other hand, Baig *et al.* [2] suggested an equation for calculating the ultimate load capacity of the columns as follows:

$$P_u = 1.10 A_c f_c + A_a f_y \tag{7}$$

in which A_c and A_a are cross-sectional areas of concrete and steel respectively, and also f_c and f_y are compressive strength of the concrete core and yield stress of the steel wall, respectively. Ultimate load capacities predicted by Equation (7) are summarised in Table 2 and compared with those values achieved from the analyses. As can be seen from the table, a mean ratio (P_u/N_u) of 1.030 is achieved with a COV of 0.039 which indicates that Equation (7) overestimates the ultimate load capacity by 3%.

Based on the obtained results summarised in Table 1 and the equation of the EC4 [11], Equation (6), an equation is also proposed for prediction of the ultimate load capacity of the stiffened CFSC stub columns in this study, as following:

$$N_B = A_a f_{yd} + 1.05 A_c f_{cd} \tag{8}$$

Predicted ultimate load capacities based on the proposed equation, Equation (8), are listed in Table 2 and compared with the ultimate load capacity values obtained from the analyses. According to the table, a mean ratio (N_B/N_u) of 0.992 is accomplished with a COV of 0.038 which demonstrates that Equation (8) gives the ultimate load capacity by only 0.8% lower than the results obtained from the nonlinear analyses. Therefore, the proposed equation of this study can give a very close prediction of the ultimate load capacity of the columns.

It is worth mentioning that ultimate load capacity predictions for eccentrically loaded columns can be done using Equations (6), (7), and (8) and the interaction curve (Figure 6.19 of EC4 [11]). These predictions based on the above-mentioned procedure for eccentrically loaded columns have been also summarised in Table 2.

Table 2 Comparison of obtained ultimate load capacity values (N_u) with predictions by EC4 [11] ($N_{pl,Rd}$), equation of Baig *et al.* [2] (P_u), and proposed equation (N_B)

No.	Column label	N_u (kN)	$N_{pl,Rd}$ (kN)	$N_{pl,Rd}/N_u$	P_u (kN)	P_u/N_u	N_B (kN)	N_B/N_u
1	C1-2.5-10-234-50-4(50)	3760	3409	0.907	3728	0.991	3584	0.953
2	C1-2.5-10-234-50-3(50)	3661	3409	0.931	3728	1.018	3584	0.979
3	C1-2.5-10-234-50-2(50)	3517	3409	0.969	3728	1.060	3584	1.019
4	C1-2.5-10-234-50-4(100)	3656	3409	0.932	3728	1.020	3584	0.980
5	C1-2.5-10-234-50-3(100)	3557	3409	0.958	3728	1.048	3584	1.008
6	C1-2.5-10-234-50-2(100)	3424	3409	0.996	3728	1.089	3584	1.047

7	C1-2.5-10-234-50-4(150)	3579	3409	0.953	3728	1.042	3584	1.001
8	C1-2.5-10-234-50-3(150)	3486	3409	0.978	3728	1.069	3584	1.028
9	C1-2.5-10-234-50-2(150)	3359	3409	1.015	3728	1.110	3584	1.067
10	C2-2.5-10-234-50-4(50)	3668	3409	0.929	3728	1.016	3584	0.977
11	C2-2.5-10-234-50-3(50)	3583	3409	0.951	3728	1.040	3584	1.000
12	C2-2.5-10-234-50-2(50)	3473	3409	0.982	3728	1.073	3584	1.032
13	C2-2.5-10-234-50-4(100)	3575	3409	0.954	3728	1.043	3584	1.003
14	C2-2.5-10-234-50-3(100)	3499	3409	0.974	3728	1.065	3584	1.024
15	C2-2.5-10-234-50-2(100)	3398	3409	1.003	3728	1.097	3584	1.055
16	C2-2.5-10-234-50-4(150)	3510	3409	0.971	3728	1.062	3584	1.021
17	C2-2.5-10-234-50-3(150)	3445	3409	0.990	3728	1.082	3584	1.040
18	C2-2.5-10-234-50-2(150)	3348	3409	1.018	3728	1.113	3584	1.071
19	C1-3-10-234-50-4(50)	3905	3499	0.896	3782	0.969	3641	0.932
20	C1-2-10-234-50-4(50)	3596	3380	0.940	3672	1.021	3526	0.981
21	C1-3-10-234-50-3(50)	3793	3499	0.922	3782	0.997	3641	0.960
22	C1-2-10-234-50-3(50)	3525	3380	0.959	3672	1.042	3526	1.000
23	C1-3-10-234-50-2(50)	3665	3499	0.955	3782	1.032	3641	0.993
24	C1-2-10-234-50-2(50)	3368	3380	1.004	3672	1.090	3526	1.047
25	C2-3-10-234-50-4(50)	3825	3499	0.915	3782	0.989	3641	0.952
26	C2-2-10-234-50-4(50)	3516	3380	0.961	3672	1.045	3526	1.003
27	C2-3-10-234-50-3(50)	3732	3499	0.938	3782	1.013	3641	0.975

Table 2 continued

No.	Column label	N_u (kN)	$N_{\text{pl,Rd}}$ (kN)	$N_{\text{pl,Rd}}/N_u$	P_u (kN)	P_u/N_u	N_B (kN)	N_B/N_u
28	C2-2-10-234-50-3(50)	3437	3380	0.983	3672	1.069	3526	1.026
29	C2-3-10-234-50-2(50)	3622	3499	0.966	3782	1.044	3641	1.005
30	C2-2-10-234-50-2(50)	3320	3380	1.018	3672	1.106	3526	1.062
31	C1-2.5-12-234-50-4(50)	3804	3409	0.896	3728	0.980	3584	0.942
32	C1-2.5-8-234-50-4(50)	3695	3409	0.923	3728	1.009	3584	0.970
33	C1-2.5-12-234-50-3(50)	3721	3409	0.916	3728	1.002	3584	0.963
34	C1-2.5-8-234-50-3(50)	3597	3409	0.948	3728	1.036	3584	0.996

35	C1-2.5-12-234-50-2(50)	3544	3409	0.962	3728	1.052	3584	1.011
36	C1-2.5-8-234-50-2(50)	3486	3409	0.978	3728	1.069	3584	1.028
37	C2-2.5-12-234-50-4(50)	3719	3409	0.917	3728	1.002	3584	0.964
38	C2-2.5-8-234-50-4(50)	3622	3409	0.941	3728	1.029	3584	0.990
39	C2-2.5-12-234-50-3(50)	3661	3409	0.931	3728	1.018	3584	0.979
40	C2-2.5-8-234-50-3(50)	3505	3409	0.973	3728	1.064	3584	1.023
41	C2-2.5-12-234-50-2(50)	3506	3409	0.972	3728	1.063	3584	1.022
42	C2-2.5-8-234-50-2(50)	3438	3409	0.992	3728	1.084	3584	1.042
43	C1-2.5-10-234-50-4(50)-30	3086	2731	0.885	2935	0.951	2834	0.918
44	C1-2.5-10-234-50-4(50)-60	2425	2114	0.872	2262	0.933	2185	0.901
45	C1-2.5-10-234-50-4(100)-30	2926	2671	0.913	2858	0.977	2759	0.943
46	C1-2.5-10-234-50-4(100)-60	2225	1996	0.897	2125	0.955	2053	0.923
47	C1-2.5-10-234-40-4(50)	3138	2860	0.911	3090	0.985	2975	0.948
48	C1-2.5-10-234-30-4(50)	2520	2285	0.907	2458	0.975	2371	0.941
49	C1-2.5-10-234-40-3(50)	3063	2860	0.934	3090	1.009	2975	0.971
50	C1-2.5-10-234-30-3(50)	2449	2285	0.933	2458	1.004	2371	0.968
51	C1-2.5-10-234-40-2(50)	2942	2860	0.972	3090	1.050	2975	1.011
52	C1-2.5-10-234-30-2(50)	2347	2285	0.974	2458	1.047	2371	1.010
53	C2-2.5-10-234-40-4(50)	3077	2860	0.929	3090	1.004	2975	0.967
54	C2-2.5-10-234-30-4(50)	2468	2285	0.926	2458	0.996	2371	0.961
55	C2-2.5-10-234-40-3(50)	3021	2860	0.947	3090	1.023	2975	0.985
56	C2-2.5-10-234-30-3(50)	2446	2285	0.934	2458	1.005	2371	0.970
57	C2-2.5-10-234-40-2(50)	2909	2860	0.983	3090	1.062	2975	1.023
58	C2-2.5-10-234-30-2(50)	2329	2285	0.981	2458	1.055	2371	1.018

Table 2 continued

No.	Column label	N_u (kN)	$N_{\text{pl,Rd}}$ (kN)	$N_{\text{pl,Rd}}/N_u$	P_u (kN)	P_u/N_u	N_B (kN)	N_B/N_u
59	C1-2.5-10-450-50-4(50)	4375	3957	0.904	4245	0.970	4101	0.937
60	C1-2.5-10-350-50-4(50)	4102	3717	0.906	4005	0.976	3861	0.941
61	C1-2.5-10-450-50-3(50)	4219	3957	0.938	4245	1.006	4101	0.972
62	C1-2.5-10-350-50-3(50)	3976	3717	0.935	4005	1.007	3861	0.971
63	C1-2.5-10-450-50-2(50)	4067	3957	0.973	4245	1.044	4101	1.008
64	C1-2.5-10-350-50-2(50)	3853	3717	0.965	4005	1.040	3861	1.002
65	C2-2.5-10-450-50-4(50)	4257	3957	0.930	4245	0.997	4101	0.963

66	C2-2.5-10-350-50-4(50)	4011	3717	0.927	4005	0.999	3861	0.963
67	C2-2.5-10-450-50-3(50)	4104	3957	0.964	4245	1.034	4101	0.999
68	C2-2.5-10-350-50-3(50)	3906	3717	0.952	4005	1.025	3861	0.989
69	C2-2.5-10-450-50-2(50)	4042	3957	0.979	4245	1.050	4101	1.015
70	C2-2.5-10-350-50-2(50)	3807	3717	0.976	4005	1.052	3861	1.014
	Mean			0.949		1.030		0.992
	SD			0.033		0.040		0.037
	COV			0.035		0.039		0.038

5 CONCLUSIONS

Behaviour of stiffened concrete-filled steel composite (CFSC) stub columns subjected to axial loading has been studied in this paper. The finite element software LUSAS was employed to carry out the non-linear finite element analyses. Accuracy of the proposed 3D finite element modelling was demonstrated by comparison of the modelling result with the corresponding experimental result. It was uncovered that the proposed modelling can predict the behaviour of the columns accurately. The CFSC stub columns were extensively developed utilising different special arrangements, number, spacing, and diameters of bar stiffeners with various steel wall thicknesses, concrete compressive strengths, and steel yield stresses. It was shown that by the use of C1 and C2 bar stiffeners the ultimate load capacity and ductility of the columns are increased. Increasing number of the bar stiffeners and/or steel wall thickness enhances the ultimate load capacity and ductility of the columns. The increase of the diameter of the bar stiffeners increases the ultimate load capacity. As spacing of the bar stiffeners decreases the ultimate load capacity and ductility are improved. The use of the bar stiffeners, increase of the number of the bar stiffeners, decrease of spacing of the bar stiffeners, enhancement of the steel wall thickness, or increase of diameter of the bar stiffeners enhances the confinement effect of the steel wall on the concrete core and delays the local buckling of the steel wall which leads to the increased ultimate load capacity and ductility. Enhancement of the load eccentricity decreases the ultimate load capacity of the columns. Also, if the concrete compressive strength is enhanced, the ultimate load capacity is increased because the use of higher concrete compressive strength significantly increases the bond strength of the columns with the stiffeners. Moreover, the higher steel yield stress results in higher ultimate load capacity. The improved ultimate load capacity of the columns owing to the increase of the concrete compressive strength and/or steel yield stress of the columns leads to utilising smaller column size and enhancing the usable floor space in a structure. The smaller size of CFSC columns results in more savings in weight and material of the structure. Meanwhile, the columns failed due to concrete crushing about their mid-height where the steel wall locally buckled. The inward buckling of the steel wall was prevented by the in-filled concrete. Based on the obtained results, an equation was also proposed to predict the ultimate load capacity of the columns. Furthermore, the ultimate load capacities of the columns were predicted based on EC4 [11], the equation of Baig *et al.* [2] and the proposed equation of this study and also compared with those obtained values from the nonlinear analyses. These comparisons revealed that the equations of EC4 [11] and Baig *et al.* [2] could respectively estimate the ultimate load capacities with 5.1% underestimation and 3% overestimation. On the other hand, the comparisons demonstrated that the proposed equation of this study could give a very close prediction of the ultimate load capacities with only 0.8% underestimation.

References

[1] A. Bahrami, W.H. Wan Badaruzzaman and S.A. Osman. Nonlinear analysis of concrete-filled steel composite columns subjected to axial loading. *Structural Engineering and Mechanics-An International Journal*, 39(3):383-398, 2011.

[2] M.N. Baig, F. Jiansheng and N. Jianguo. Strength of concrete filled steel tubular columns. *Tsinghua Science and Technology*, 11(6):657-666, 2006.

[3] C.G. Bailey. Fire engineering design of steel structures. *Advances in Structural Engineering*, 8(3): 185–202, 2005.

[4] M.A. Dabaon, M.H. El-Boghdadi and M.F. Hassanein. Experimental investigation on concrete-filled stainless steel stiffened tubular stub columns. *Engineering Structures,* 31:300-307, 2009.

[5] M. Dabaon, S. El-Khoriby, M. El-Boghdadi and M.F. Hassanein. Confinement effect of stiffened and unstiffened concrete-filled stainless steel tubular stub columns. *Journal of Constructional Steel Research*, 65:1846-1854, 2009.

[6] X.H. Dai and D. Lam. Shape effect on the behaviour of axially loaded concrete filled steel tubular stub columns at elevated temperature. *Journal of Constructional Steel Research*, 73:117–127, 2012.

[7] E. Ellobody and B. Young. Design and behaviour of concrete-filled cold-formed stainless steel tube columns. *Engineering Structures*, 28:716-728, 2006a.

[8] E. Ellobody and B. Young. Nonlinear analysis of concrete-filled steel SHS and RHS columns. *Thin-Walled Structures*, 44:919–930, 2006b.

[9] E. Ellobody, B. Young and D. Lam. Behaviour of normal and high strength concrete-filled compact steel tube circular stub columns. *Journal of Constructional Steel Research*, 62(7):706-715, 2006.

[10] A. Elremaily and A. Azizinamini. Behavior and strength of circular concrete-filled tube columns. *Journal of Constructional Steel Research*, 58:1567-1591, 2002.

[11] Eurocode 4, BS EN 1994-1-1. Design of composite steel and concrete structures- Part 1-1: General rules and rules for buildings. *London: British Standard Institutio*n, 2004.

[12] Finite Element Analysis Ltd., *LUSAS User's Manual, Version 14*, Surrey, UK, 2006.

[13] G. Giakoumelis and D. Lam. Axial capacity of circular concrete-filled tube columns. *Journal of Constructional Steel Research*, 60(7):1049–1068, 2004.

[14] C.D. Goode and D. Lam. Concrete-filled steel tube columns–tests compared with Eurocode 4. *Proceedings of the international conference on composite construction VI*, Devil's Thumb Ranch, Colorado, USA, July 20-24, 2008.

[15] L.H. Han, W. Liu and Y.F. Yang. Behaviour of concrete-filled steel tubular stub columns subjected to axially local compression. *Journal of Constructional Steel Research*, 64:377-387, 2008.

[16] L.H. Han, Y.F. Yang and L. Xu. An experimental study and calculation on the fire resistance of concrete-filled SHS and RHS columns. *Journal of Constructional Steel Research,* 59:427–452, 2003.

[17] L.H. Han, G.H. Yao and X.L. Zhao. Tests and calculations for hollow structural steel (HSS) stub columns filled with self-consolidating concrete (SCC). *Journal of Constructional Steel Research*, 61:1241-1269, 2005.

[18] L.H. Han, X.L. Zhao, Y.F. Yang and J.B. Feng. Experimental study and calculation of fire resistance of concrete-filled hollow steel columns, *Journal of Structural Engineering, ASCE*, 129(3):346-356, 2003.

[19] H.T. Hu, C.S. Huang and Z.L. Chen. Finite element analysis of CFT columns subjected to an axial compressive force and bending moment in combination. *Journal of Constructional Steel Research*, 61:1692–1712, 2005.

[20] H.T. Hu, C.S. Huang, M.H. Wu and Y.M. Wu. Nonlinear analysis of axially loaded concrete-filled tube columns with confinement effect. *Journal of Structural Engineering ASCE*, 129(10):1322–1329, 2003.

[21] H.T. Hu and W.C. Schnobrich. Constitutive modeling of concrete by using nonassociated plasticity. *Journal of Materials in Civil Engineering*, 1(4):199–216, 1989.

[22] V.K.R. Kodur. Performance of high strength concrete-filled steel columns exposed to fire. *Canadian Journal of Civil Engineering*, 25:975-981, 1998.

[23] V.K.R. Kodur, F.P. Cheng, T.C. Wang and M.A. Sultan. Effect of strength and fibre reinforcement on fire resistance of high-strength concrete columns. *Journal of Structural Engineering, ASCE*, 129(2):253-259, 2003.

[24] D. Lam and L. Gardner. Structural design of stainless steel concrete filled columns. *Journal of Constructional Steel Research*, 64(11):1275-1282, 2008.

[25] T.T. Lie and V.K.R. Kodur. Fire resistance of steel columns filled bar-reinforced concrete. *Journal of Structural Engineering, ASCE*, 122(1):30-36, 1996.

[26] J.Y.R. Liew and D.X. Xiong. Effect of preload on the axial capacity of concrete-filled composite columns. *Journal of Constructional Steel Research*, 65:709-722, 2009.

[27] M.L. Lin and K.C. Tsai. Behaviour of double-skinned composite steel tubular columns subjected to combined axial and flexural loads. *Proceedings of the first international conference on the steel & composite structures*. Pusan, Korea, 1145-1152, 2001.

[28] D. Liu, W.M. Gho and J. Yuan. Ultimate capacity of high-strength rectangular concrete-filled steel hollow section stub columns. *Journal of Constructional Steel Research*, 59: 1499-1515, 2003.

[29] H. Lua, X.L. Zhaoa and L.H. Han. Testing of self-consolidating concrete-filled double skin tubular stub columns exposed to fire, *Journal of Constructional Steel Research*, 66:1069-1080, 2010.

[30] J.B. Mander, M.J.N. Priestley and R. Park. Theoretical stress–strain model for confined concrete. *Journal of Structural Engineering ASCE*, 114(8):1804-1826, 1988.

[31] M.A. Mansur, M.S. Chin and T.H. Wee. Stress-strain relationship of high-strength fiber concrete in compression. *Journal of Materials in Civil Engineering*, 11(1):21-29, 1999.

[32] S. Morino and K. Tsuda. Design and construction of concrete-filled steel tube column system in Japan. *Earthquake Engineering and Engineering Seismology,* 4(1): 51-73, 2003.

[33] G. Muciaccia, F. Giussani, G. Rosati and F. Mola. Response of self-compacting concrete filled tubes under eccentric compression. *Journal of Constructional Steel Research*, 67:904-916, 2011.

[34] M. Mursi. The behaviour and design of thin walled concrete filled steel box columns. *Ph.D. Thesis. School of Civil and Environmental Engineering, The University of New South Wales*, Sydney, Australia, 2007.

[35] M. Mursi and B. Uy. Strength of concrete filled steel box columns incorporating interaction buckling. *Journal of Structural Engineering ASCE*, 129(5): 626–639, 2003.

[36] W.L.A. Oliveira, S. De Nardin, A.L.H.C. El Debs and M.K. El Debs. Evaluation of passive confinement in CFT columns. *Journal of Constructional Steel Research*, 66:487-495, 2010.

[37] F.E. Richart, A. Brandzaeg and R.L. Brown. A study of the failure of concrete under combined compressive stresses. *Bull. 185, Champaign, IL, USA: University of Illinois Engineering Experimental Station,* 1928.

[38] M.L. Romero, V. Moliner, A. Espinos, C. Ibañez and A. Hospitaler. Fire behavior of axially loaded slender high strength concrete-filled tubular columns, *Journal of Constructional Steel Research*, 67: 1953–1965, 2011.

[39] L.P. Saenz. Discussion of "Equation for the stress–strain curve of concrete" by P. Desayi and S. Krishnan, *Journal of the American Concrete Institute*, 61(3):1229–1235, 1964.

[40] P. Schaumann, V.K.R. Kodur and O. Bahr. Fire behaviour of hollow structural section steel columns filled with high strength concrete, *Journal of Constructional Steel Research*, 65:1794-1802, 2009.

[41] Z. Tao, L.H. Han and D.Y. Wang. Experimental behaviour of concrete-filled stiffened thin-walled steel tubular columns. *Thin-Walled Structures*, 45:517-527, 2007.

[42] Z. Tao, L.H. Han and Z.B. Wang. Experimental behaviour of stiffened concrete-filled thin-walled hollow steel structural (HSS) stub columns. *Journal of Constructional Steel Research*, 61:962-983, 2005.

[43] Z. Tao, B. Uy, L.H. Han and Z.B. Wang. Analysis and design of concrete-filled stiffened thin-walled steel tubular columns under axial compression. *Thin-Walled Structures*, 47: 1544-1556, 2009.

[44] M. Tomii. Ductile and strong columns composed of steel tube infilled concrete and longitudinal steel bars. Special volume, *Proceedings of the third international conference on steel–concrete composite structures.* Fukuoka, Japan: Association of Steel-Concrete Structures, 1991.

[45] K. Uenaka, H. Kitoh and K. Sonoda. Concrete filled double skin circular stub columns under compression. *Thin-Walled Structures*, 48:19-24, 2010.

[46] B. Uy and S.B. Patil. Concrete-filled high strength steel box columns for tall buildings: behaviour and design. *Structural Design of Tall Buildings*, 5:75–94, 1996.

[47] B. Uy, Z. Tao and L.H. Han. Behaviour of short and slender concrete-filled stainless steel tubular columns. *Journal of Constructional Steel Research*, 67:360-378, 2011.